Research Square

Preprints are preliminary reports that have not undergone peer review.
They should not be considered conclusive, used to inform clinical practice,
or referenced by the media as validated information.

Traffic-Induced Energy Variability of Long-Haul Truck Powertrains Using Vehicle–Traffic Co-Simulation

Abhilasha Saroj
sarojaj@ornl.gov
Oak Ridge National Laboratory
Anye Zhou
Oak Ridge National Laboratory
Guanhao Xu
Oak Ridge National Laboratory
Safi Ebeid
Mission College
Vivek Sujan
Oak Ridge National Laboratory
Michael O. Rodgers
Oak Ridge National Laboratory
Oriana Calderón
University of Tennessee at Knoxville
Chieh (Ross) Wang
Oak Ridge National Laboratory

Research Article

Keywords: Freight energy, long-haul simulation, traffic microsimulation, electric truck, co-simulation

Posted Date: September 8th, 2026

DOI: https://doi.org/10.21203/rs.3.rs-10629719/v1

License: This work is licensed under a Creative Commons Attribution 4.0 International License.
Read Full License

Additional Declarations: No competing interests reported.

Traffic-Induced Energy Variability of Long-Haul Truck Powertrains Using Vehicle–Traffic Co-Simulation

Abhilasha Saroj[1*], Anye Zhou[1], Guanhao Xu[1], Safi Ebeid[3], Vivek Sujan[1], Michael O. Rodgers[1], Oriana Calderón[2], Chieh (Ross) Wang[1]

[1*]Oak Ridge National Laboratory, 1 Bethel Valley Road, Oak Ridge, 37830, TN, USA.
[2]Department of Civil and Environmental Engineering, University of Tennessee, Knoxville, 37996, TN, USA.
[3]Mission College, Santa Clara, California, USA.

*Corresponding author(s). E-mail(s): sarojaj@ornl.gov;

Abstract

Long-haul freight energy evaluation requires models that capture corridor-scale traffic dynamics and vehicle-level powertrain behavior. This paper provides methodology to evaluate a Class 8 truck on a 255-mile section of the U.S. Interstate 81 (I-81) corridor using vehicle–traffic co-simulation under spatiotemporally varying demand. To reduce computational cost, we use a two-stage design. Stage 1 develops a SUMO microscopic simulation for eight factorial scenarios defined by season, weekday type, and time of day, with multiple random seeds. Second-by-second ego-truck trajectories provide travel-time and selected-route energy-intensity estimates. Time of day most clearly separates traffic-flow regimes. Beta-distribution fits show that PM scenarios have more irregular speed profiles and weaker histogram-based fit ($\boldsymbol{R^2 = 0.499}$–$\boldsymbol{0.758}$), whereas AM scenarios show more stable free-flow behavior and stronger fit ($\boldsymbol{R^2 = 0.950}$–$\boldsymbol{0.984}$); seasonal effects are comparatively small. Stage 2 therefore evaluates selected summer weekday AM and PM cases using SUMO–IPG TruckMaker© co-simulation with a physics-based battery-electric truck model. Relative to a no-traffic baseline, traffic increases energy intensity by 23%–53%, reduces freight efficiency by 22%–37%, and increases regenerative-energy fraction by 104%–165%. The results demonstrate the importance of coupling realistic traffic variability with high-fidelity powertrain modeling for long-haul freight energy assessment.

Keywords: Freight energy, long-haul simulation, traffic microsimulation, electric truck, co-simulation.

1 Introduction

High-fidelity vehicle–traffic co-simulation is increasingly needed to evaluate the real-world energy effects of long-haul freight operations, where second-by-second speed trajectories, congestion, and interactions with surrounding traffic can strongly influence fuel and energy use [1–3]. Traffic microsimulation can represent network-level congestion and vehicle interactions, but often lacks detailed powertrain dynamics. Physics-based vehicle modeling can resolve second-by-second energy behavior in greater detail, but it usually lacks realistic traffic interactions. Vehicle–traffic co-simulation, linking realistic traffic interactions with high-fidelity vehicle and powertrain dynamics, therefore, has the potential to provide more realistic evaluation [3, 4]. Simulation-based freight energy studies address this problem from complementary perspectives, including planning-scale long-haul electrification analysis, microsimulation-based trajectory energy estimation, and vehicle/powertrain simulation. These approaches often emphasize regional freight-energy impacts, traffic-flow dynamics, or detailed vehicle physics separately. Recent integrated simulation frameworks connect traffic and vehicle-level modeling, but relatively few corridor-scale long-haul freight studies jointly represent spatiotemporally varying demand and high-fidelity co-simulation [3–6]. This gap reflects both modeling and computational challenges. Developing realistic long-haul traffic scenarios requires substantial data integration, demand generation, and calibration effort, while applying physics-based vehicle models in co-simulation over long corridors with ambient traffic and many stochastic demand scenarios is computationally expensive [3, 4]. Motivated by these challenges, this study addresses three research questions:

1. **Methodology at scale:** What are the practical steps, data needs, and key challenges in building a 255-mile Interstate 81 (I-81) freeway microsimulation network with realistic traffic demand using public data and open-source tools?
2. **Impact of traffic demand variability:** How do time-of-day, weekday/weekend, and seasonal demand variations affect long-haul travel time and energy use, and which factor should be prioritized in freight energy evaluation?
3. **Value of co-simulation:** How much additional insight does vehicle-level co-simulation provide compared with energy estimates derived from microsimulation trajectories alone?

[0]This work was supported by the US Department of Energy (DOE), Office of Critical Minerals and Energy Innovation, Transportation Technologies Office under Award Number DE-EE0009857. (Corresponding author: Abhilasha Saroj.) This manuscript has been authored by UT-Battelle, LLC, under contract DE-AC05-00OR22725 with the US Department of Energy (DOE). The US government retains and the publisher, by accepting the article for publication, acknowledges that the US government retains a nonexclusive, paid-up, irrevocable, worldwide license to publish or reproduce the published form of this manuscript, or allow others to do so, for US government purposes. DOE will provide public access to these results of federally sponsored research in accordance with the DOE Public Access Plan (https://www.energy.gov/doe-public-access-plan).

We develop and demonstrate a two-stage framework for corridor-scale energy evaluation of emerging freight powertrains under realistic traffic variability. In Stage 1, a microscopic traffic simulation of the I-81 corridor is developed in *Simulation of Urban MObility* (SUMO), an open-source simulator that supports agent-based traffic modeling and high-resolution vehicle trajectory outputs for energy and emissions analysis [7]. Time-varying traffic demand is generated across season, weekday type, and time of day, and the resulting microsimulation scenarios are evaluated using travel time, speed-distribution, and trajectory-based energy metrics. This analysis identifies time of day as the scenario dimension producing the clearest separation in traffic-flow and energy-relevant driving behavior, with PM conditions showing longer travel times and more variable speed profiles than AM conditions.

In Stage 2, representative AM and PM scenarios are evaluated using vehicle–traffic co-simulation over a 255-mile corridor section. The co-simulation couples SUMO with IPG TruckMaker© through the Real-Sim Flexible Interface for X-in-the-loop Simulation (FIXS) [8], enabling high-fidelity vehicle and powertrain behavior to be evaluated under realistic surrounding traffic conditions. This staged design reduces the number of computationally expensive co-simulation runs while preserving the ability to quantify traffic-induced energy-use variability under realistic long-haul operating conditions.

Contributions. This paper makes three contributions. First, it presents a transferable workflow for developing simulation of a long freight corridor using public traffic data, including Federal Highway Administration (FHWA) Highway Performance Monitoring System (HPMS) [9] Annual Average Daily Traffic (AADT) and FHWA Traffic Monitoring and Analysis Stations (TMAS) hourly counts [10]. Second, it develops a scenario-based experimental design to quantify how season, weekday type, and time of day affect long-haul travel time, speed distributions, and trajectory-based energy intensity, and uses the results to identify time of day as the primary driver of corridor-scale traffic and energy variability in the studied scenarios. Third, it evaluates selected AM and PM scenarios using vehicle–traffic co-simulation with a physics-based battery-electric Class 8 truck model, quantifying traffic-induced changes in energy intensity, freight efficiency, and regenerative-energy recovery relative to a no-traffic baseline.

2 Related Work

2.1 Microscopic simulation and trajectory-based energy and emissions modeling

Microscopic traffic simulation is widely used to generate second-by-second vehicle trajectories that support energy, fuel, and emissions estimation beyond average-speed methods[11–14]. By accounting for high-resolution localized interactions, including acceleration patterns, car-following behavior, and intersection control dynamics, microsimulation helps bridge the gap between aggregate traffic data and instantaneous environmental impacts [12, 15]. These models allow practitioners to extract detailed speed and acceleration profiles, which serve as inputs to vehicle-specific instantaneous fuel-consumption and emissions models that macroscopic frameworks typically smooth out [11, 15]. SUMO is a widely used open-source microsimulator that supports detailed trajectory output together with integrated emissions and energy models such

as PHEMlight and PHEMlight5 [7, 16, 17]. Trajectory-based modeling is important because energy and emissions depend strongly on transient driving behavior, including acceleration, deceleration, and stop-and-go conditions. A representative instantaneous model is VT-Micro, which relates fuel and emissions to speed and acceleration and has been validated against measured data [18, 19].

2.2 Vehicle–traffic co-simulation for vehicle-level energy fidelity

Although trajectory-based models are useful for estimating energy and emissions from microscopic simulation outputs, they may not capture detailed vehicle physics such as grade effects, traction limits, powertrain control, thermal constraints, and regenerative braking. Vehicle–traffic co-simulation addresses this limitation by coupling microscopic traffic flow with higher-fidelity vehicle dynamics and powertrain models. Real-Sim FIXS enables this multiresolution coupling between traffic simulators and vehicle/virtual-environment components [8]. Recent work also shows that elevation and detailed longitudinal dynamics can materially affect energy outcomes, particularly for heavy-duty and electric vehicles [20]. Related studies have examined energy-aware cooperative on-ramp merging using SUMO/SIMULINK joint simulation [21], real-time online speed replanning using vehicle–traffic–communication co-simulation [22], and incentive mechanisms for cooperative merging using multi-agent deep reinforcement learning [23].

2.3 Corridor-scale traffic scenario generation

Corridor-scale microsimulation remains challenging because it requires consistent network generation, data fusion, demand development, calibration, and substantial computational effort. Prior large-scale studies have shown feasibility but also highlighted the workflow burden of building day-long microscopic models for major regions [24]. To operationalize microscopic simulation at scale, recent research focuses on structured model-development workflows and cross-platform alignment. A three-tier incremental framework guides the transition from offline, history-driven models to real-time, data-driven traffic digital twins [25]. Because reproducible simulation studies may require different simulation engines, subsequent work evaluates scenario consistency across independent platforms [26]. Building on this direction, the Real-Twin framework [27, 28] automates multi-source data ingestion to generate consistent microscopic simulation environments across SUMO, VISSIM, and AIMSUN. Such workflows are important for long-haul freight energy studies because corridor-scale operating conditions, demand patterns, and traffic variability shape the trajectories that are later used for energy estimation or co-simulation.

2.4 Regional freight energy and infrastructure analysis

At a broader planning scale, freight energy studies increasingly examine corridor infrastructure, operating constraints, and regional deployment pathways for emerging heavy-duty powertrains. Recent work has linked freight mobility, traffic, weather, and energy systems to evaluate heavy-duty charging and hydrogen infrastructure deployment [29–32]. These studies complement microsimulation and co-simulation approaches by

addressing regional energy demand, infrastructure siting, charging/refueling requirements, grid impacts, and system-level planning needs. In contrast, high-resolution traffic simulation and vehicle–traffic co-simulation provide more detailed insight into how local traffic conditions, vehicle interactions, and transient speed profiles affect vehicle-level energy performance.

3 Corridor Microsimulation Model and Scenario Generation

3.1 Real-Twin

In this effort, Real-Twin [27, 28] is used to develop the I-81 microscopic traffic simulation model by integrating roadway-network information, traffic demand data, and simulator-specific configuration files into a consistent scenario-generation workflow. The resulting scenarios represent time-varying traffic demand across season, weekday type, and time of day using the public data sources described in Section 3.2. These scenarios support evaluation of demand-variability effects on corridor travel time, speed distributions, and trajectory-based energy estimates, and they provide representative operating conditions for subsequent vehicle–traffic co-simulation.

The generated I-81 network also incorporates corridor elevation information. Elevation is especially important for freight energy evaluation because roadway grade directly affects tractive power demand, vehicle speed response, regenerative braking opportunities, and battery-electric truck energy consumption. Prior work shows that raw elevation data can contain noise, discontinuities, and abrupt grade changes that may have limited effects in conventional traffic simulation but can strongly affect vehicle dynamics and energy estimates in co-simulation [20]. That study examines these issues on an I-81 corridor segment and proposes an elevation-processing workflow that smooths unrealistic artifacts while preserving roadway geometry, improving the realism and stability of vehicle–traffic co-simulation [20]. Hence, this study includes elevation-aware network generation to support more realistic long-haul freight powertrain energy evaluation.

3.2 Traffic Demand

The traffic demand model combines two public data sources: Annual Average Daily Traffic (AADT) from Federal Highway Administration's (FHWA) Highway Performance Monitoring System (HPMS) [9] and hourly vehicle counts from FHWA's Traffic Monitoring Analysis System (TMAS) [10]. HPMS AADT provides the baseline 24-hour demand along the I-81 corridor, including mainline volumes, on-ramp inflows, and off-ramp outflows. TMAS hourly counts provide scenario-specific scaling factors that capture hourly demand variation by time of day (TOD), season, and weekday type.

3.2.1 Estimating Missing AADT and Truck Shares on I-81 Segments

Because the modeled corridor crosses Virginia, West Virginia, Maryland, and Pennsylvania, HPMS AADT data are assembled from all four states [33–36]. Some sources report total AADT together with truck AADT or truck percentage, whereas others report only aggregate AADT. Figure 1 illustrates these differences using sample I-81 AADT points from West Virginia and Pennsylvania.

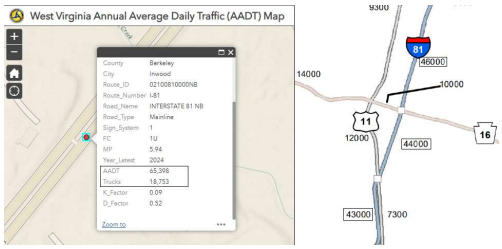


Fig. 1 Sample AADT data points on I-81 in West Virginia and Pennsylvania.

Missing total AADT values are estimated using local flow-balance consistency between consecutive mainline segments. Differences between upstream and downstream mainline AADT represent the net effect of nearby ramp inflows and outflows. The same principle supports missing truck AADT estimation when truck counts or truck percentages are unavailable. Truck-share estimates are further constrained using patterns observed in the available data. Reported truck percentages do not exceed 30%, and nearby paired on-ramp and off-ramp truck shares are generally similar. Therefore, missing truck percentages are selected to remain below 30%, maintain similar values for nearby ramp pairs, and preserve local consistency in both total AADT and truck AADT across adjacent mainline and ramp segments.

3.2.2 Scenario Factors from TMAS: Time of Day, Season, and Weekday Type

TMAS hourly counts are used to convert baseline AADT into scenario-specific demand volumes. For each TMAS station, scaling factors are computed for scenarios defined by season, weekday type, and time-of-day (TOD) window. Let $T(d, h)$ denote the vehicle count on day d during hour h. Let D_{all} be the set of all valid days in the year, D_{season} the set of valid days in a given season, $D_{\text{day}} \subset D_{\text{season}}$ the subset of seasonal days matching the selected weekday type, and H_{tod} the set of hours in the selected TOD window. Let N_{all} and N_{day} denote the number of days in D_{all} and D_{day}, respectively.

The annual average daily volume at a station is computed as

$$T_{\text{all}} = \frac{1}{N_{\text{all}}} \sum_{d \in D_{\text{all}}} \sum_{h=1}^{24} T(d, h). \tag{1}$$

The average TOD-window volume for the selected season and weekday type is computed as

$$T_{\text{season,day,tod}} = \frac{1}{N_{\text{day}}} \sum_{d \in D_{\text{day}}} \sum_{h \in H_{\text{tod}}} T(d,h). \tag{2}$$

This formulation applies the temporal filtering sequentially. The set of days is first restricted to the selected season, then to the selected weekday type within that season, and finally to the hours belonging to the selected TOD window. Therefore, $T_{\text{season,day,tod}}$ is computed only from days that satisfy both the selected season and weekday-type conditions.

The station-level scenario factor is computed as

$$F = \frac{T_{\text{season,day,tod}}}{T_{\text{all}}}. \tag{3}$$

Thus, F represents the fraction of annual average daily volume assigned to the selected TOD window under the specified seasonal and weekday-type conditions at that station. These factors are computed for each station, scenario, and vehicle class where class-specific counts are available. The resulting factors are used to scale the baseline AADT and truck AADT estimates developed in Section 3.2.1.

Because TMAS stations are spatially sparse along I-81, applying a single station factor to the full corridor would not preserve local demand variation. Therefore, the network is divided into directional zones using consecutive TMAS stations as boundaries. As shown in Figure 2, each zone extends between two neighboring TMAS stations. For each scenario, the zone factor Z is computed as the average of the two bounding station factors:

$$Z = \frac{F_A + F_B}{2}, \tag{4}$$

where F_A and F_B are the upstream and downstream station-level scenario factors, respectively. The resulting zone factor is applied to all baseline AADT values, including truck AADT where available, within the corresponding zone.

3.3 Automatic Traffic Demand Ingestion in SUMO

3.3.1 Mapping Ramp-Level Demand Estimates to SUMO Flow Inputs

A key step in long-corridor demand generation is mapping estimated ramp-level inflow volumes to the correct SUMO network edge IDs. This step is challenging because demand inputs are organized by ramp name or location, whereas SUMO requires vehicle flows to be assigned to specific network edges. To support semi-automated demand ingestion, we use a graph-based procedure that links ramp AADT estimates, TMAS-based scenario factors, and hourly flow inputs.



Fig. 2 Partition of the northbound I-81 network into directional zones using TMAS stations as boundaries. Blue dots indicate TMAS station locations, and orange segments indicate the resulting zones.

The mapping workflow proceeds through four steps: identifying ramp-related SUMO edge IDs, linking ramp names to those edge IDs, assigning each ramp to a TMAS-based demand zone, and writing scenario-specific SUMO flow inputs.

- **Graph-based edge identification:** A directed graph uses the SUMO `.net.xml` file and NetworkX [37]. The northbound (NB) and southbound (SB) directions form separate directional subnetworks. For each direction, the dominant backbone path represents the mainline. Edges that merge into the backbone represent on-ramps, and edges that diverge from it represent off-ramps. This step identifies the SUMO edge IDs needed for ramp inflows and exit split ratios.
- **Ramp-name to edge-ID matching:** SUMO ramp edge IDs are matched to OpenStreetMap ramp names because the demand spreadsheets index ramp volumes by ramp name. This mapping assigns on-ramp AADT estimates to the correct inflow edges and off-ramp AADT estimates to the correct exit edges.
- **TMAS zone assignment:** TMAS stations divide the corridor into directional demand zones so that each ramp receives an appropriate scenario factor Z. Coordinate-based nearest-neighbor matching links each TMAS station to the nearest SUMO junction. Consecutive matched stations define zone boundaries, and the NetworkX graph identifies the corridor edges within each zone. Each ramp receives the zone factor computed from the two bounding TMAS stations.
- **Scenario flow-file generation:** Scenario-specific SUMO flow files define demand by direction and vehicle class. For each on-ramp, the corresponding zone factor Z scales the baseline AADT. The resulting hourly demand is written to the `vehsPerHour` attribute of a SUMO `flow` element, with one entry for each hour in the selected TOD window.

This procedure converts spatially resolved ramp AADT estimates and TMAS-based temporal scaling factors into SUMO-compatible hourly inflows for trucks and nontrucks across the modeled I-81 corridor.

3.3.2 Split Ratio Ingestion and Scenario Generation

After scenario-specific ramp inflows are generated, exit split ratios are computed and written to a SUMO turn-ratio file. These split ratios define the probability that vehicles leave the mainline at each off-ramp and provide the routing inputs needed to generate scenario- and seed-specific vehicle routes.

- **Exit split-ratio estimation:** Exit probabilities are computed from the AADT-based demand sheet. For each off-ramp, the exit probability is the ratio of off-ramp AADT to the upstream mainline AADT immediately preceding the exit:

$$P_{\text{off}} = \frac{\text{AADT}_{\text{off-ramp}}}{\text{AADT}_{\text{upstream mainline}}}. \tag{5}$$

  SUMO turn-ratio definitions store the resulting P_{off} values in the `.turn.xml` file.
- **Route generation:** The SUMO `jtrrouter` tool generates scenario- and seed-specific route files by combining the flow file, turn-ratio file, vehicle-type definitions, and random seed.
- **Scenario configuration:** A scenario-specific `.sumocfg` file references the network file, route file, and additional files, and specifies the simulation time window, step length, and random seed.

3.4 Model Verification and Validation

The simulation model covers a 358-mile I-81 corridor, while the energy evaluation focuses on a selected 255-mile route within this network. Model verification is performed for the full 358-mile corridor to ensure that the broader traffic simulation operates consistently before extracting the energy-analysis route. Verification includes repeated checks of the simulation network against real-world corridor characteristics, including the number of lanes, lane additions and drops, speed limits, lane widths, and the locations of true on- and off-ramps. Figure 3 shows the modeled I-81 corridor in SUMO together with a representative ego truck used in the co-simulation environment. In addition to geometric verification, the network is evaluated under the estimated demand inputs to identify unrealistic traffic behavior. Because corridor demand is estimated rather than directly observed, some local adjustments are required. For example, recurring bottlenecks are observed near certain ramps where very short mainline segments immediately upstream of off-ramps or downstream of on-ramps restrict merging and diverging maneuvers, creating artificial congestion. To mitigate these artifacts while preserving corridor-level flow consistency, AADT is redistributed from problematic ramps to nearby comparable ramps.

For preliminary validation, we compare the simulated end-to-end travel time of a representative Class 8 ego truck with Google Maps travel time estimates for the same I-81 route in both northbound (NB) and southbound (SB) directions. The comparison uses the `all_year_weekday_1PM-9PM` scenario, representing typical weekday traffic conditions between 1 and 9 p.m. Because observed truck travel time data are not available, Google Maps time ranges are used as an external reference to assess the reasonableness of simulated corridor travel times.

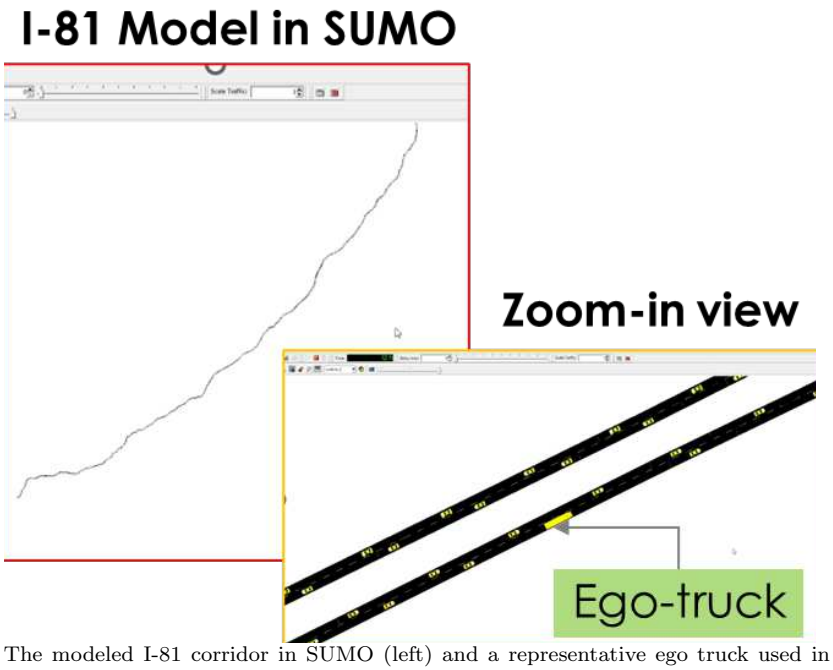


Fig. 3 The modeled I-81 corridor in SUMO (left) and a representative ego truck used in the co-simulation environment (inset).

The simulated travel times for both directions fall within the corresponding Google Maps ranges. The NB trip takes 5 h 59 min, compared with a Google Maps estimate of 5 h to 6 h 10 min, whereas the SB trip takes 6 h 3 min, compared with an estimate of 5 h 10 min to 6 h 10 min. These results provide an initial corridor-level check that the calibrated model yields reasonable travel times for the selected scenario, although validation against observed probe or truck trajectory data is still needed.

4 Truck Powertrain Model Development and Co-Simulation Setup

4.1 Truck Powertrain Model

The vehicle modeled in the co-simulation environment is a battery-electric truck (BET), representing a high-efficiency Class 8 freight powertrain configuration used to evaluate traffic-induced energy-performance variability. The selected aerodynamic, rolling-resistance, trailer, and payload parameters reflect an advanced high-efficiency BET configuration rather than the full range of commercially deployed Class 8 trucks. Therefore, the absolute energy-intensity values should be interpreted as configuration-specific. However, because the same BET model is held fixed across all evaluated traffic conditions, the comparative results remain useful for isolating the effect of traffic variability on powertrain energy performance.

The BET uses a 6×4 driveline configuration, with two front steering wheels and four driven rear wheels distributed across two rear axles. Two electric motors, one mounted on each rear axle, provide a combined maximum driving torque of 2,200 Nm.

Each rear axle is paired with a three-speed automatic transmission, with gear ratios of 5.6, 2.8, and 1.4 for the first, second, and third gears, respectively.

The BET is equipped with a 700 kWh high-voltage battery to support uninterrupted simulation over the I-81 corridor. The battery operates at 660 V, with the state of charge constrained between 20% and 80%. The maximum battery power is set to 1,600 kW.

A sequential regenerative braking strategy is implemented to recover braking energy. Regenerative braking is applied first through the electric motors. Friction braking is introduced only when the braking torque demand exceeds the available regenerative braking torque by more than 10 Nm. The minimum braking torque is set to 2 Nm, and regenerative braking is enabled only above a minimum vehicle speed of 2 km/h.

A two-axle trailer is configured to pair with the BET tractor. The tractor and trailer both have an air-drag coefficient of 0.325 at 10 m^2 frontal area. The rolling resistance coefficients are as follows: tractor steering tires, 0.0041; tractor driving tires, 0.004; and trailer tires, 0.0036. The gross combined weight of BET is 79,093 lb, consisting of a 25,618 lb tractor, an 11,475 lb trailer, and a 42,000 lb payload.

To navigate the BET in traffic, an intelligent driver model-based longitudinal controller is incorporated to plan safe speed in traffic. A proportional-integral-feedforward controller then modulates the truck throttle/brake to execute the planned speed. The lateral controller from IPG TruckMaker is adopted to control tractor steering for keeping the BET in the desired lane (obtained from a prespecified routing configuration).

4.2 Co-Simulation Setup

The co-simulation framework combines SUMO, IPG TruckMaker, Simulink, and Oak Ridge National Laboratory's (ORNL's) Real-Sim to capture both ambient traffic interactions and high-fidelity ego-truck dynamics (as shown in Fig. 4).

SUMO simulates surrounding traffic on the selected corridor segment with calibrated car-following and lane-changing models. Although suitable for corridor-scale traffic flow, SUMO does not capture detailed vehicle dynamics and BET powertrain characteristics needed for high-fidelity energy analysis, such as traction limits, regenerative braking, and detailed energy consumption. Thus, the ego Class 8 BET is modeled in IPG TruckMaker, which provides detailed vehicle dynamics and powertrain simulation.

Real-Sim provides synchronization between SUMO and IPG TruckMaker, enabling bidirectional interaction between the ego truck and the surrounding traffic. This setup allows the ego BET to affect surrounding traffic while also responding to realistic traffic conditions to preserve physics-based vehicle dynamics for energy-related evaluation.

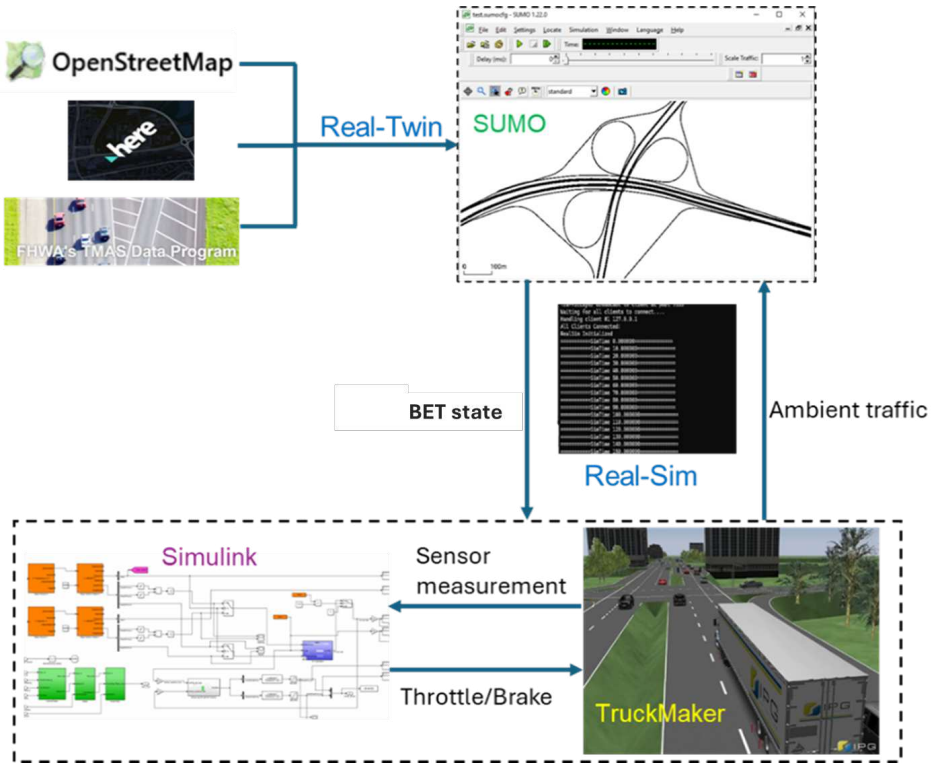


Fig. 4 vehicle–traffic co-simulation framework.

5 Experimental Design

5.1 Scenario Matrix and Two-Stage Study Design

The analysis follows a two-stage design to quantify how temporal demand variability affects corridor-scale travel time and truck energy outcomes.

Stage 1 evaluates a full microsimulation scenario matrix defined by three temporal dimensions: **season** (summer [S], winter [W]), **day type** (weekday [WD], weekend [WE]), and **time of day** (AM: 1–9 a.m.; PM: 1–9 p.m.). Scenario labels follow the order `Season--DayType--TOD`; for example, `SWDAM` denotes summer weekday a.m., and `WWEPM` denotes winter weekend p.m. The full factorial design yields eight scenarios: `SWDAM`, `SWDPM`, `SWEAM`, `SWEPM`, `WWDAM`, `WWDPM`, `WWEAM`, and `WWEPM`. Each scenario is simulated with 10 random seeds to capture stochastic variability in traffic interactions and route realization, resulting in 80 microsimulation runs.

Each Stage 1 run includes one ego vehicle representing a **Class 8 truck** traversing the full modeled corridor. The ego-truck trajectory is recorded at 1 Hz and supports two complementary analyses. First, end-to-end **travel time** is evaluated over the full corridor. Second, **energy consumption** and **energy intensity** are evaluated on a **selected route** within the corridor that is of specific interest to the truck vendor. The same selected route is also used in Stage 2 co-simulation.

5.2 Trajectory-Based Energy Evaluation in Stage 1

Energy is estimated from the simulated trajectory using the *general tractive energy* formulation implemented in MOVESTAR. First, MOVESTAR computes tractive power demand from instantaneous speed, acceleration, rolling resistance, and aerodynamic drag, then it integrates power over time to obtain total energy consumption [38]. Energy intensity is reported as trip energy divided by trip distance (kWh/mile). This trajectory-based formulation directly maps traffic-induced changes in speed variability, stop-and-go behavior, and delay into changes in vehicle energy demand [38].

Stage 1 results identify the temporal factors that contribute most to variability in full-corridor travel time and selected-route energy outcomes. Stage 2 then downselects representative scenarios for higher-fidelity vehicle–traffic co-simulation. This downselection is necessary because co-simulation requires tighter coupling time steps and more detailed vehicle dynamics, making evaluation of all 80 cases computationally very expensive at corridor scale.

6 Results

6.1 Stage 1: Microsimulation Results

Stage 1 evaluates the eight scenarios—`SWDAM`, `SWDPM`, `SWEAM`, `SWEPM`, `WWDAM`, `WWDPM`, `WWEAM`, and `WWEPM`—with 10 random seeds per scenario. Across the Stage 1 results, the clearest separation is between **a.m.** and **p.m.** conditions. The p.m. scenarios produce higher travel times, larger dispersion, and higher selected-route energy use than those produced by the a.m. scenarios. This behavior is consistent with travel-time reliability guidance showing stronger variability during peak-period conditions [39, 40]. Energy follows the same pattern because it is sensitive to transient speed and acceleration behavior, especially under stop-and-go traffic [18, 19, 41].

Selected-route travel time (Fig. 5). Fig. 5 shows selected-route travel-time distributions for the Class 8 ego truck across the eight Stage 1 scenarios. Across all runs, the mean travel time is 4.56 h, and the standard deviation is 0.57 h, with values ranging from 3.83 to 6.33 h. The strongest separation occurs by time of day: all p.m. scenarios have higher medians than the a.m. scenarios, and the summer p.m. cases—`SWDPM` and `SWEPM`—show the largest travel times and widest spreads. In contrast, the four a.m. scenarios cluster tightly around 4.0–4.1 h with limited variability. Season and day type act as secondary modifiers within the p.m. regime, but the dominant effect is the a.m.–p.m. split, with p.m. travel times averaging 30–40% longer than their a.m. counterparts.

Selected-route energy and energy intensity (Fig. 6). Fig. 6 reports energy consumption (kilowatt-hours) and energy intensity (kilowatt-hours/mile) on the selected route. Across all runs, mean selected-route energy consumption is 927.134 kWh (standard deviation: 115.161 kWh), and mean selected-route energy intensity is 3.594 kWh/mile (standard deviation: 0.446 kWh/mile). The same a.m.–p.m. separation appears in the energy results. The p.m. scenarios consistently show higher selected-route energy use and higher energy intensity than that of a.m. scenarios, indicating that congestion and speed variability increase both total energy demand

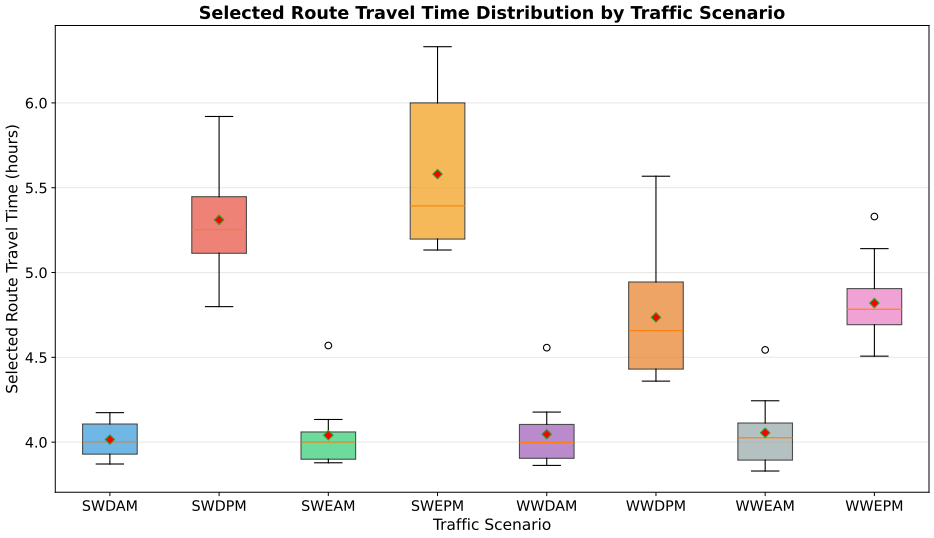


Fig. 5 Selected-route travel time distributions across eight Stage 1 traffic scenarios.

and per-mile energy use. The largest selected-route energy levels occur under `SWDPM`, `SWEPM`, and `WWDPM`, whereas the a.m. scenarios remain lower and more tightly grouped. This direction is consistent with prior work showing that congestion and stop-and-go operation increase fuel and energy consumption [18, 19, 41].

Speed distributions and Beta fits (Fig. 7). To summarize ego-truck speed variability, Beta distributions are fit to pooled speed samples (0–70 mph) from the 10 seeds within each scenario. Fig. 7 shows a clear regime difference. The a.m. scenarios, `SWDAM`, `SWEAM`, `WWDAM`, and `WWEAM`, are strongly concentrated near free-flow speed, with most probability mass near the upper end of the range and only a modest lower-speed tail. In contrast, the p.m. scenarios, `SWDPM`, `SWEPM`, `WWDPM`, and `WWEPM`, are broader and assign substantially more mass to lower speeds, consistent with intermittent congestion in addition to free-flow operation. The fitted parameter pairs separate these regimes clearly: a.m. scenarios cluster at large α with β close to 1, whereas p.m. scenarios cluster at much smaller α and lower β, indicating qualitatively different speed-distribution shapes.

Goodness-of-fit and regime separation (Fig. 8). Fig. 8 reports two complementary fit measures for the Beta speed model. Quantile-based R^2 assesses how well the model captures the overall empirical distribution shape and remains high across all scenarios (0.866–0.972), indicating good agreement at the distribution level. Histogram-based R^2 evaluates bin-level density agreement and is more sensitive to local shape mismatch, multimodality, and boundary effects. This metric is also high for a.m. scenarios (0.950–0.984), showing that a single Beta distribution represents mostly free-flow conditions well but drops substantially for p.m. scenarios (0.499–0.758), indicating a poorer fit under mixed free-flow and congested states. The parameter-space plot shows the same pattern: a.m. scenarios cluster in a high-fit region, whereas p.m. scenarios form a distinct lower-α, lower-β group. Overall, these results identify time

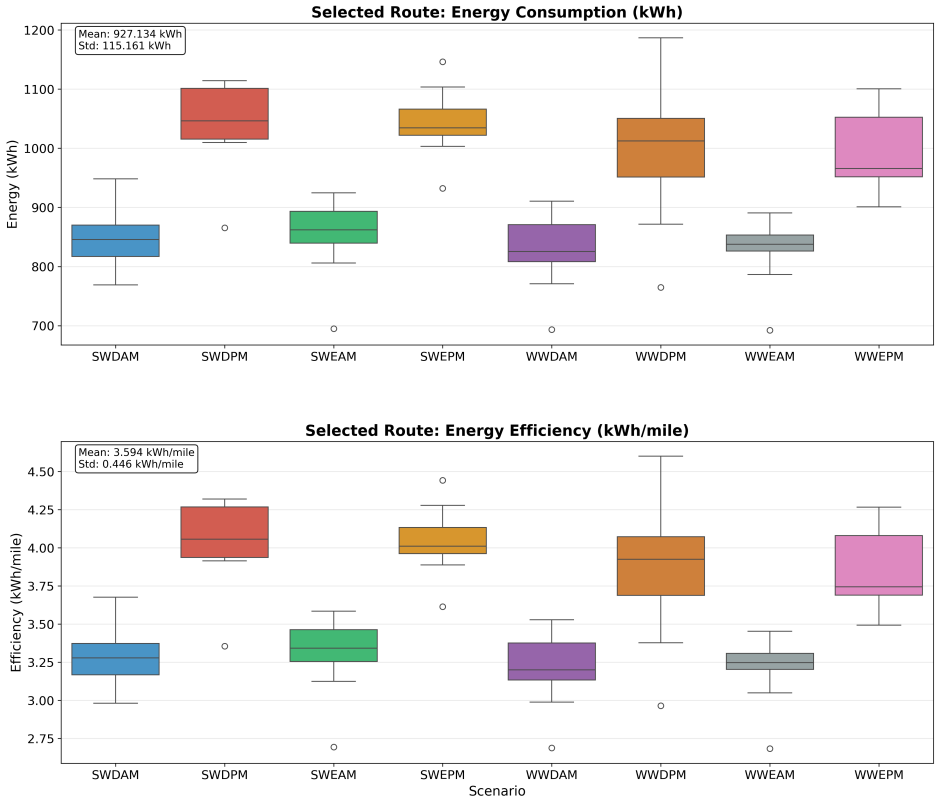


Fig. 6 Selected-route energy consumption and energy intensity across Stage 1 scenarios.

of day as the primary driver of speed-regime separation, with season and day type having smaller, secondary effects.

Based on the Stage 1 results, `SWDAM` and `SWDPM` are selected for Stage 2 because they capture the dominant a.m.–p.m. operating-regime contrast. Stage 2 focuses on the same selected route as that used in the Stage 1 energy analysis and evaluates each scenario with two random seeds using higher-fidelity vehicle–traffic co-simulation for a **Class 8 BET**.

6.2 Stage 2: Co-Simulation Results

Stage 2 applies the high-fidelity vehicle–traffic co-simulation to quantify how ambient traffic affects long-haul **Class 8 BET** truck energy performance.

Co-simulation is performed for the NB direction of the selected 255-mile I-81 corridor segment. Two Stage 1 scenarios are evaluated (i.e., `SWDAM` and `SWDPM`), and each scenario is simulated with two random seeds. A no-traffic baseline is also simulated to isolate the effect of ambient traffic interactions.

Table 1 reports BET energy intensity (kilowatt-hour/mile), freight efficiency (ton-mile/kilwatt-hour), and regenerative-energy fraction. Relative to the no-traffic

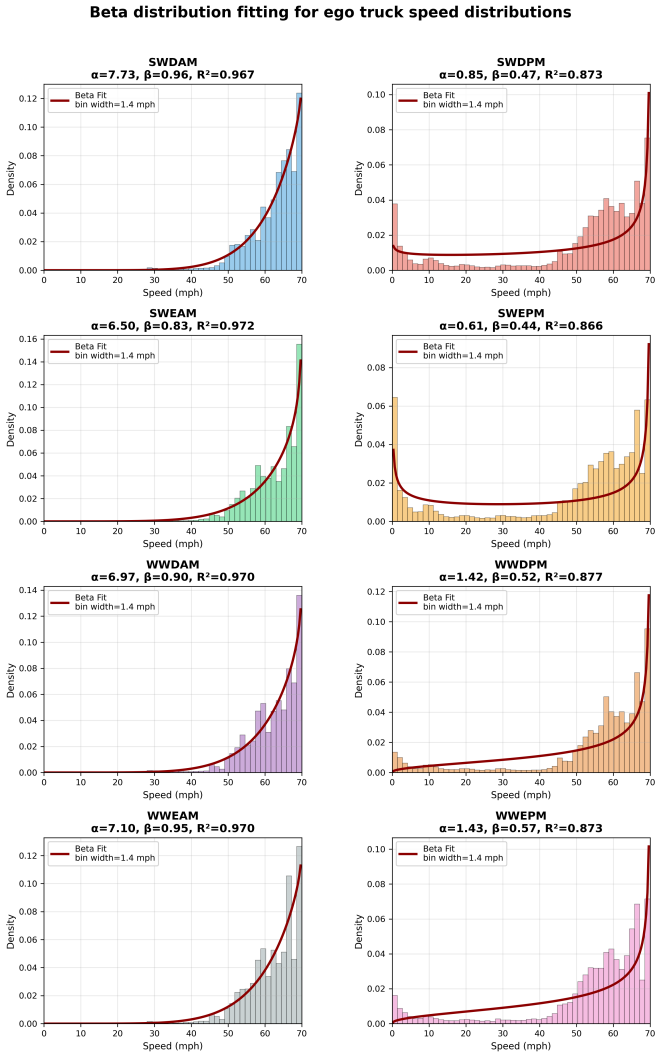


Fig. 7 Beta distribution fits to pooled ego-truck speed samples for each Stage 1 scenario. The R^2 values shown in each panel correspond to quantile-based R^2.

baseline, both `SWDAM` and `SWDPM` increase energy use and reduce freight efficiency. Ambient traffic introduces more stop-and-go behavior and greater speed variability, which increase traction energy demand. At the same time, the regenerative fraction increases because the BET experiences more frequent coasting and braking in response to slower traffic and queue formation.

Fig. 9 summarizes the percent change in these metrics relative to the no-traffic baseline. The higher-demand `SWDPM` case produces the largest degradation, with energy consumption increasing by up to 53% and freight efficiency decreasing by up to 37%.

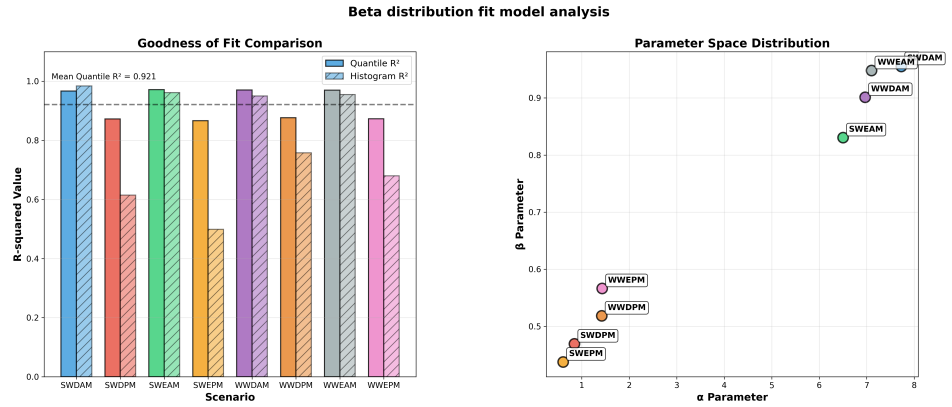


Fig. 8 Beta fit diagnostics across Stage 1 scenarios.

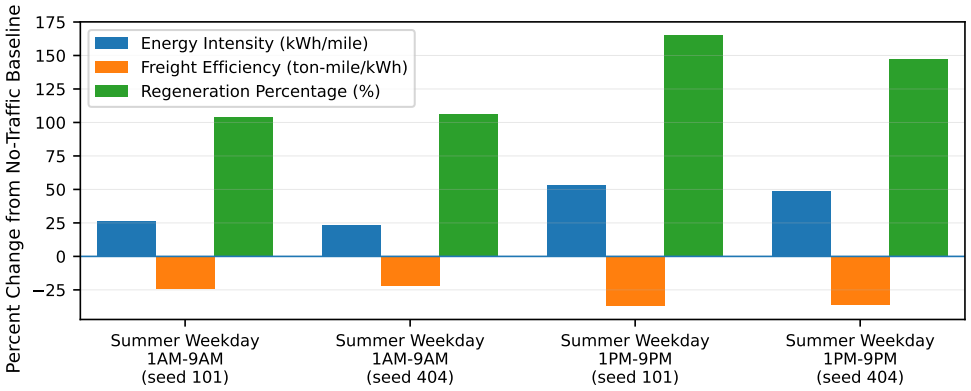


Fig. 9 Percent change in co-simulation metrics relative to the no-traffic baseline for `SWDAM` and `SWDPM`, each evaluated with two random seeds.

Across all cases, the regenerative fraction increases substantially (104%–165%), reflecting more frequent deceleration and greater opportunity for energy recovery. These results show that realistic ambient traffic conditions materially affect long-haul BET truck energy performance and should be represented in corridor-scale freight energy analysis.

7 Discussion and Conclusion

The results support a clear two-stage interpretation. Stage 1 microsimulation provides an efficient way to screen a broad scenario space and identify the traffic conditions that matter most for truck performance. Across the eight scenarios, the dominant factor is **time of day**: p.m. scenarios consistently produce higher full-corridor travel times, larger dispersion, and higher selected-route energy use than those of a.m. scenarios.

Table 1 BET co-simulation efficiency results. Percent changes are relative to the no-traffic baseline.

Scenario	kWh/mi	ton-mi/kWh	Regen (%)
Baseline (no traffic)	2.08	9.14	8.78
`SWDAM` (seed 101)	2.63 (+26%)	6.91 (-24%)	17.9 (+104%)
`SWDAM` (seed 404)	2.56 (+23%)	7.09 (-22%)	18.1 (+106%)
`SWDPM` (seed 101)	3.18 (+53%)	5.70 (-37%)	23.3 (+165%)
`SWDPM` (seed 404)	3.10 (+49%)	5.85 (-36%)	21.7 (+147%)

Season and day type act mainly as secondary modifiers. The fitted Beta speed distributions reinforce this result. The a.m. scenarios are concentrated near free-flow speeds and are represented well by a single Beta distribution, whereas p.m. scenarios exhibit broader low-speed components and lower histogram-based fit quality, indicating more complex mixed traffic states.

Stage 2 co-simulation confirms that these traffic differences materially affect BET performance on the selected route. Relative to the no-traffic baseline, ambient traffic increases energy intensity by 23%–53%, reduces freight efficiency by 22%–37%, and increases regenerative-energy fraction by 104%–165%. The larger regenerative fraction shows that congested traffic creates more braking and recovery opportunities, but these gains do not offset the additional traction demand caused by stop-and-go operation and speed fluctuations. The `SWDPM` case produces the largest penalty, consistent with the Stage 1 result that p.m. conditions represent the more energy-intensive operating regime. Overall, the proposed workflow combines the scalability of microsimulation-based trajectory analysis with the fidelity of vehicle–traffic co-simulation.

8 Limitations and Future Work

A key limitation of this study is the limited number of vehicle–traffic co-simulation runs that could be completed because of the high computational cost of simulating a very long corridor with a high-fidelity physics-based vehicle model. As a result, the co-simulation-based energy consumption and energy efficiency results should be interpreted as initial evidence rather than fully converged estimates, and additional runs across more scenarios and seeds are needed to establish robustness and quantify the extent of improvement over microsimulation-only results. Future work should therefore focus on improving computational efficiency through approaches such as distributed computing, hybrid simulation architectures, surrogate-assisted evaluation, or selective high-fidelity simulation of the most informative scenarios.

Another limitation is that the microsimulation model could not be rigorously calibrated to observed driving behavior, travel times, and speed distributions because of limited ground-truth field data and the difficulty of calibrating a network of this scale. Although the model captures reasonable system-level patterns, stronger calibration using richer observed trajectory, speed, and travel-time data would improve confidence in both mobility and energy-related results. Future work should investigate scalable calibration strategies and expanded data collection to strengthen behavioral realism.

Finally, the battery electric truck physics model could not be directly validated against real-world operational data because such data were not available for the study corridor and vehicle configuration. This limits confidence in the absolute powertrain energy estimates, even though the model is useful for comparative scenario analysis. Future work should incorporate empirical heavy-duty BET performance data, when available, to validate and refine the vehicle model under realistic operating conditions.

Funding Declaration

This work was supported by the US Department of Energy (DOE), Office of Critical Minerals and Energy Innovation, Transportation Technologies Office under Award Number DE-EE0009857.

Consent to Publish

Consent to Publish declaration: not applicable.

Ethics and Consent to Participate

Ethics and Consent to Participate declarations: not applicable.

Acknowledgments

This work was supported by the US Department of Energy (DOE), Office of Critical Minerals and Energy Innovation, Transportation Technologies Office under Award Number DE-EE0009857. The authors thank Volvo Group, NA for providing data and insights. The authors thank Gage Adams, Jessica Grillo, and Nicholas Kurzak for their contributions through the U.S. Department of Energy Office of Science's Science Undergraduate Laboratory Internships (SULI) and Community College Internships (CCI) programs at Oak Ridge National Laboratory.

Author Contributions

A.S., A.Z., M.O.R., V.S., and C.R.W. contributed to the study conception and design. A.S., A.Z., G.X., S.E., V.S., M.O.R., C.R.W. contributed to data collection and model development. A.S., A.Z., M.O.R., V.S., C.R.W. contributed to the analysis and interpretation of results. A.S., A.Z., and S.E. prepared the original manuscript draft. All authors reviewed and revised the manuscript, reviewed the results, and approved the final version of the manuscript.

Competing Interests

The authors declare no competing interests.

Legal Disclaimer

This report was prepared as an account of work sponsored by an agency of the United States Government. Neither the United States Government nor any agency thereof, nor any of its employees, makes any warranty, express or implied, or assumes any legal liability or responsibility for the accuracy, completeness, or usefulness of any information, apparatus, product, or process disclosed, or represents that its use would not infringe privately owned rights. Reference herein to any specific commercial product, process, or service by trade name, trademark, manufacturer, or otherwise does not necessarily constitute or imply its endorsement, recommendation, or favoring by the United States Government or any agency thereof. The views and opinions of authors expressed herein do not necessarily state or reflect those of the United States Government or any agency thereof.

References

[1] Ahn, K., Rakha, H., Trani, A., Van Aerde, M.: Estimating vehicle fuel consumption and emissions based on instantaneous speed and acceleration levels. Journal of Transportation Engineering **128**(2), 182–190 (2002) https://doi.org/10.1061/(ASCE)0733-947X(2002)128:2(182)

[2] Barth, M.J., Boriboonsomsin, K.: Real-world carbon dioxide impacts of traffic congestion. Transportation Research Record: Journal of the Transportation Research Board **2058**(1), 163–171 (2008) https://doi.org/10.3141/2058-20

[3] Shao, Y., Chambon, P., Cook, A., Wang, R., Deter, D.: Evaluating connected and automated vehicles in co-simulation environment of traffic microsimulation and vehicle dynamics. In: 2023 IEEE Intelligent Vehicles Symposium (IV). IEEE, ??? (2023). https://doi.org/10.1109/IV55152.2023.10186617

[4] Varga, B., Doba, D., Tettamanti, T.: Optimizing vehicle dynamics co-simulation performance by introducing mesoscopic traffic simulation. Simulation Modelling Practice and Theory **124**, 102739 (2023) https://doi.org/10.1016/j.simpat.2023.102739

[5] Tong, F., Wolfson, D., Jenn, A., Scown, C.D., Auffhammer, M.: Energy consumption and charging load profiles from long-haul truck electrification in the united states. Environmental Research: Infrastructure and Sustainability **1**(2), 025007 (2021) https://doi.org/10.1088/2634-4505/ac186a

[6] Fu, Y., Chen, Y.: An integrated traffic and powertrain simulation framework to evaluate fuel efficiency impacts of fully and partial vehicle automation. Sustainability **17**(12), 5527 (2025) https://doi.org/10.3390/su17125527

[7] Behrisch, M., Bieker, L., Erdmann, J., Krajzewicz, D.: SUMO – Simulation of Urban MObility: An Overview. In: Proceedings of SIMUL 2011, The Third International Conference on Advances in System Simulation (2011)

[8] Shao, Y., Deter, D., Cook, A., *et al.*: Real-sim interface: Enabling multi-resolution simulation and x-in-the-loop development for connected and automated vehicles. SAE International Journal of Connected and Automated Vehicles **5**(4), 327–339 (2022) https://doi.org/10.4271/12-05-04-0026

[9] Federal Highway Administration: Highway Performance Monitoring System (HPMS). https://www.fhwa.dot.gov/policyinformation/hpms.cfm. Office of Highway Policy Information. Accessed: May 12, 2026 (2026)

[10] Federal Highway Administration: Special Tabulations / U.S. Traffic Volume Data. https://www.fhwa.dot.gov/policyinformation/tables/tmasdata/. Travel Monitoring Analysis System (TMAS) traffic volume data. Office of Highway Policy Information. Accessed: May 12, 2026 (2026)

[11] Osorio, C., Nanduri, K.: Energy-efficient urban traffic management: A microscopic simulation-based approach. Transportation Science **49**(3), 637–651 (2015) https://doi.org/10.1287/trsc.2014.0554

[12] Oskarbski, J., Biszko, K.: Estimation of vehicle energy consumption at intersections using microscopic traffic models. Energies **16**(1), 233 (2023) https://doi.org/10.3390/en16010233

[13] Saroj, A., Roy, S., Guin, A., Hunter, M., Fujimoto, R.: Smart city real-time data-driven transportation simulation. In: Proceedings of the Winter Simulation Conference, pp. 857–868 (2018)

[14] Saroj, A.J., Roy, S., Guin, A., Hunter, M.: Development of a connected corridor real-time data-driven traffic digital twin simulation model. Journal of Transportation Engineering, Part A: Systems **147**(12) (2021) https://doi.org/10.1061/JTEPBS.0000599

[15] Osorio, C., Nanduri, K.: Urban transportation emissions mitigation: Coupling high-resolution vehicular emissions and traffic models for traffic signal optimization. Transportation Research Part B: Methodological **81**, 520–538 (2015) https://doi.org/10.1016/j.trb.2014.12.007

[16] Eclipse SUMO / DLR: Emissions – SUMO Documentation. Accessed 2026-02-27. https://sumo.dlr.de/docs/Models/Emissions.html

[17] Eclipse SUMO / DLR: PHEM (Passenger Car and Heavy Duty Emission Model) / PHEMlight – SUMO Documentation. Accessed 2026-02-27. https://sumo.dlr.de/docs/Models/Emissions/PHEMlight.html

[18] Ahn, K., Rakha, H., Trani, A., Van Aerde, M.: Estimating vehicle fuel consumption and emissions based on instantaneous speed and acceleration levels. Journal of Transportation Engineering **128**(2), 182–190 (2002) https://doi.org/10.1061/(ASCE)0733-947X(2002)128:2(182)

[19] Rakha, H., Ahn, K., Trani, A.: Development of VT-Micro model for estimating hot stabilized light duty vehicle and truck emissions. Transportation Research Part D: Transport and Environment **9**(1), 49–74 (2004) https://doi.org/10.1016/S1361-9209(03)00054-3

[20] Xu, G., Zhou, A., Saroj, A.J., Wang, C.R., Sujan, V., Rodgers, M.O., Chen, J., Calderón, O., Wang, Z.: Incorporating elevation in traffic-vehicle co-simulation: Issues, impacts, and solutions. 2025 Winter Simulation Conference (WSC), 1023–1034 (2025)

[21] Wang, Z., Zhou, A., Cook, A., Shao, Y., Xu, G., Chen, J.M.: Energy-centric cooperative onramp merging strategy: An analytical solution. In: 2023 IEEE International Automated Vehicle Validation Conference (IAVVC), pp. 1–7 (2023). https://doi.org/10.1109/IAVVC57316.2023.10328114

[22] Wang, Z., Zhou, A., Cook, A., Chen, J., Xu, G., Shao, Y.: Cooperative merging via online speed replanning: A model-free approach with vehicle-to-vehicle communication packet drop compensation. IEEE Transactions on Intelligent Transportation Systems **26**(11), 18894–18905 (2025) https://doi.org/10.1109/TITS.2025.3591736

[23] Zhou, A., Wang, Z., Beck, J., Cook, A.: Incentivizing cooperative merging control: Insights from multi-agent deep reinforcement learning. IFAC-PapersOnLine **59**(3), 103–108 (2025) https://doi.org/10.1016/j.ifacol.2025.07.018

[24] Xiong, C., Zhu, Z., He, X., Chen, X., Zhu, S., Mahapatra, S., Chang, G.-L., Zhang, L.: Developing a 24-hour large-scale microscopic traffic simulation model for the before-and-after study of a new tolled freeway in the washington, dc–baltimore region. Journal of Transportation Engineering **141**(6), 05015001 (2015)

[25] Saroj, A., Roy, S., Guin, A., Hunter, M.: A three-tier incremental approach for development of smart corridor digital twins. In: 2023 IEEE 26th International Symposium on Real-Time Distributed Computing (ISORC), pp. 214–219 (2023). https://doi.org/10.1109/ISORC58943.2023.00038

[26] Saroj, A., Xu, G., Shao, Y., Wang, C.R.: A systematic comparison for consistent scenario development using microscopic simulation software. In: Proceedings of the 2024 Winter Simulation Conference, pp. 194–205 (2024). https://doi.org/10.1109/WSC63780.2024.10838810

[27] Xu, G., Saroj, A., *et al.*: Developing an automated microscopic traffic simulation scenario generation tool. Transportation Research Record **2679**(11), 650–672 (2025)

[28] Wang, C., Xu, G., Saroj, A., Luo, X., Yuan, J., Shao, Y.: Real-Twin. Computer Software (2025). https://doi.org/10.11578/dc.20250602.3 . https://github.com/ORNL-Real-Sim/Real-Twin

[29] Sujan, V., Sun, R., Jatana, G., Fan, J.: Hydrogen and electric charging infrastructure for heavy-duty trucks: A nationally scalable megaregion assessment. In: WCX SAE World Congress Experience. SAE International, ??? (2025). https://doi.org/10.4271/2025-01-8608

[30] Borlaug, B., et al.: Charging needs for electric semi-trailer trucks. Renewable and Sustainable Energy Transition **2** (2022) https://doi.org/10.1016/j.rset.2022.100038

[31] McNeil, W.H., Tong, F., Harley, R.A., Auffhammer, M., Scown, C.D.: Corridor-level impacts of battery-electric heavy-duty trucks and the effects of policy in the united states. Environmental Science & Technology **58**(1) (2023) https://doi.org/10.1021/acs.est.3c05139

[32] Powell, B., Johnson, C., Yip, A., Snelling, A.: Electric medium- and heavy-duty vehicle charging infrastructure attributes and development. Technical Report NREL/TP-5R00-91571, National Renewable Energy Laboratory (NREL) (2024). https://docs.nrel.gov/docs/fy25osti/91571.pdf

[33] Virginia Department of Transportation: Virginia Traffic Volume Interactive Map. Web Mapping Application. Accessed: September 15, 2025 (2025). https://www.arcgis.com/apps/webappviewer/index.html?id=35e4c06de0f84a9c9f3fe18e67cd2c92

[34] West Virginia Department of Transportation: West Virginia AADT Dataset. Accessed: September 15, 2025 (2024). https://gis.transportation.wv.gov/aadt/

[35] Maryland Department of Transportation State Highway Administration: MDOT SHA Annual Average Daily Traffic (AADT). Maryland's GIS Data Catalog (MD iMAP). Accessed: September 15, 2025 (2025). https://data.imap.maryland.gov/datasets/maryland::mdot-sha-annual-average-daily-traffic-aadt/explore

[36] Pennsylvania Department of Transportation: Statewide 2024 Traffic Volume Map (AADT). Report, Bureau of Planning and Research, Transportation Planning Division (2024). Accessed: September 15, 2025. https://gis.penndot.pa.gov/BPR_PDF_FILES/MAPS/Traffic/Traffic_Volume/Statewide/Statewide_2024_tv.pdf

[37] Hagberg, A.A., Schult, D.A., Swart, P.J.: Exploring network structure, dynamics, and function using networkx. In: Varoquaux, G., Vaught, T., Millman, J. (eds.) Proceedings of the 7th Python in Science Conference, pp. 11–15 (2008)

[38] Wang, Z., Wu, G., Scora, G.: MOVESTAR: An Open-Source Vehicle Fuel and Emission Model based on USEPA MOVES (2021). https://arxiv.org/abs/2008.04986

[39] Culotta, K., et al.: Does travel time reliability matter? a primer. Technical Report FHWA-HOP-19-062, Federal Highway Administration (FHWA), Office

of Operations (2019). https://ops.fhwa.dot.gov/publications/fhwahop19062/fhwahop19062.pdf

[40] Morris, P., Hale, D.K., Semeja, N.: Travel time reliability reference guide. Technical Report FHWA-HOP-21-015, Federal Highway Administration (FHWA), Office of Operations (2023). https://ops.fhwa.dot.gov/publications/fhwahop21015/fhwahop21015.pdf

[41] Barth, M., Boriboonsomsin, K.: Real-world carbon dioxide impacts of traffic congestion. Transportation Research Record **2058**(1), 163–171 (2008) https://doi.org/10.3141/2058-20